Analysis and evaluation of structural properties of Co_3O_4 microparticles obtained at low temperature

L. J. Cardenas-Flechas[1]*, J. J. Barba-Ortega[2], M. R. Joya[2]
[1]Universidad Nacional de Colombia, Facultad de Ingeniería, Departamento de Ingeniería Mecánica y Mecatrónica, Grupo de Física Mesoscópica, Calle 45 #30-03, Bogotá, Colombia
[2]Universidad Nacional de Colombia, Facultad de Ciencias, Departamento de Física, Grupo de Física Mesoscópica, Bogotá, Colombia

Abstract

In the present research, the synthesis of cobalt oxide Co_3O_4 was carried out using the sol-gel technique with subsequent heat treatment at 225 and 235 °C. The final product obtained was characterized by X-ray diffraction (XRD), showing a pure crystalline phase of Co_3O_4, cell parameters a=b=c=8.071 Å, and a volume of 525.7 Å^3. The particle size was between 2.37 and 2.77 μm, which indicated that structural transformations from Co to Co_3O_4 induced an increase in the particle size. Through Rietveld refinement, the interatomic distances and inclination angles of the Co_1, Co_2, and Co_3 polyhedra were analyzed in order to establish the structural behavior of cobalt oxide (II, III) at 235 °C. The UV-vis analysis allowed determining band gap (E_g) with values of 1.6 eV in the first region and 0.97 eV in the second. Scanning electron microscopy images showed that the particles agglomerated with increasing calcination temperature and exhibited larger particles. This work presents a detailed analysis of structural parameters of Co_3O_4 using the Vesta software with Rietveld refinement data.
Keywords: Co_3O_4, synthesis, structural parameters, polyhedra.

INTRODUCTION

Transition metal oxides in the nano-size regime show many size-dependent optical, electronic, magnetic, and chemical properties. Cobalt spinel (II, III) or Co_3O_4 is one of the most studied oxides since its atoms have shown efficient activity and stability in different media [1]. Cobalt oxide (II, III) is the thermodynamically stable form of cobalt oxide at room temperature and partial pressure of oxygen, with ferrimagnetism and Néel temperature starting from approximately 40 K [2, 3]. Co_3O_4 nanostructures and their nanocomposites have been extensively used as an efficient electrode material with various electrochemical applications, such as detection of water contaminants, including phenol-based compounds, dyes, salts, pesticides, molecule detection, metals, toxins produced by bacteria, etc. [4]. Some of their advantages are the high response, simple electronic measurement, and compatibility with electronic devices. Recent studies analyze the behavior of Co_3O_4 with 5-hydroxymethylfurfural (HMF) adsorption [5], Co_3O_4@ MOF-74 nanocomposites as an electrochemical sensor [6] such as lithium-ion battery (LIB) anodes [7] as well as doping with other elements like Sn [8] and Ni [9].

The Co_3O_4 has been synthesized by various methods including the sol-gel technique [10] that allowed obtaining other unique characteristics and advantages such as good electrochemical performance and stability of the structure such as mesoporous octahedra [11]. Assisted sol-gel by polymers is employed, for the production of materials with controlled nanostructure, using polypropylene, collagen, among others [12]. The core of most of these applications lies in the ability to adjust the shape and size of the morphology on which depends the electronic, magnetic, electrochemical, and catalytic properties of the cobalt oxide particles [13]. Non-spherical particles provide various morphologies and topographies, surface atom densities, surface steps, folds, and edges. Many of these morphologies allow a greater surface area feasible for different applications thanks to the nano-sized grains [14], including nano-sized geometries to control the behavior of their properties [15]. These factors lead to different physicochemical properties of the particles, even for the same chemical composition [16, 17]. The structural properties of compounds such as cobalt oxide (II, III) allow establishing the behavior of these systems, thanks to their morphology, chemical composition, and grain size. Therefore, this research analyzes the refinement parameters of the Co_3O_4 obtained by the calcined sol-gel technique at 225 and 235 °C. The parameters analyzed were the main interatomic distances of the compound bonds, volumes of the polyhedra as well as Wyckoff positions, and the lattice parameter that was calculated through the analytical approach and the Rietveld refinement. In the literature, there are few previous works related to the analysis of structural parameters of the compound Co_3O_4 obtained by the sol-gel technique when there is a variation in temperature.

EXPERIMENTAL

The synthesis was carried out using the sol-gel

*ljcardenasf@unal.edu.co
https://orcid.org/0000-0001-6039-3924

method with 21.82 g of cobalt nitrate tetrahydrate as reagent [$Co(NO_3)_2.6H_2O$, ≥99%, Merck) and 13.12 cm^3 of ethanol (C_2H_5OH, 96%, Merck) as a solvent with a 1:3 precursor:solvent ratio with constant stirring and then pre-calcination to remove moisture. The powders were removed from the oven and ground for a short time with little force; these samples turned purple. Subsequently, they were brought to a final heat treatment at 225 and 235 °C.

The X-ray diffraction analysis (XRD) was performed in a diffractometer (X'pert Pro, PANalytical), with data taken at an angle of 2θ between 10° and 80°, using an RTMS (real time multiple strip) detector with CuKα radiation at a wavelength of 1.542 Å and a step size of 0.0263° in Bragg-Brentano mode. The GSAS II code was used for Rietveld's refinement of the experimental data. The UV-vis reflectance spectrum was measured with a spectrometer (Cary 5000 UV-Vis-NIR, Agilent) in diffuse reflectance mode in the 200-2500 nm wavelength range. The morphological analysis was performed with a scanning electron microscope (SEM, Quanta 200, FEI) in secondary electron mode in a high vacuum with a voltage of 30 kV. The calculation of the particle size was carried out with the SEM images, with a count through the ImageJ software. The qualitative chemical composition analysis was done by means of energy-dispersive spectroscopy (EDS).

RESULTS AND DISCUSSION

Stoichiometric and non-stoichiometric oxides have been developed from cobalt oxide, implying a mixed valence of cobalt and the presence of oxygen vacancies [18]. Cobalt forms three oxides: cobalt monoxide (CoO), cobalt oxide (Co_2O_3), and tricobalt tetroxide (Co_3O_4). Commercial oxides are usually mixtures of the above. Other techniques have been used to obtain cobalt oxides with higher valence such as CoO_2 [19], and other composite structures for CoO_3 [20]. Fig. 1 shows the crystallographic structures of some cobalt oxides: CoO [21], CoO_2 [22], CoO_3 [20], and Co_3O_4 [23]. This oxide has a complex electronic structure reflected in the cobalt photoemission at the cobalt nucleus level, as well as in its valence [19]. Spinel cobalt oxide or Co_3O_4 has a normal structure with octahedrally coordinated Co^{3+} and tetrahedrally coordinated Co^{2+}. This oxide undergoes the antiferromagnetic phase transition.

Fig. 2 shows the XRD patterns of the samples obtained: a) $Co(CO_3)_{0.5}(OH).0.11H_2O$ (denoted as Co1); and $CoCO_3$-Co1 calcined at: b) 225 °C, and c) 235 °C. For (a), several peak**s** were observed corresponding to the precursors used in the sol-gel synthesis that include cobalt acetate and ethanol, as indicated in the experimental details indexed in JCPDS files 48-008 and 11-0692, respectively [24]. In (b) and (c), the peaks shown corresponded to the calcined samples that coincided with the Co_3O_4 spinel structure with code COD 01-074-1656 in positions 2θ of 19.04°, 31.34°, 36.93°, 38.64°, 44.92°, 49.20°, 55.79°, 59.51°, 65.40°, 68.81°, 69.92°, 74.32°, 77.55°, and 78.62°. These peaks were associated with the planes (111), (220), (311), (222), (400),
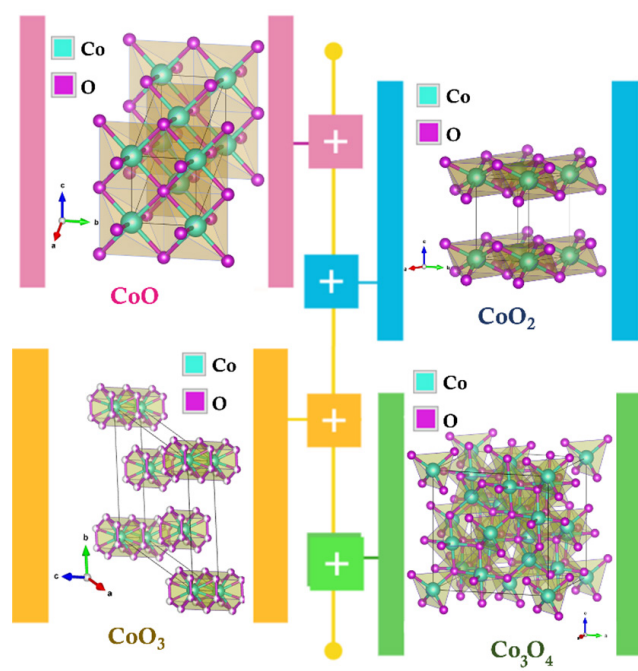

Figure 1: Crystallographic structures of cobalt oxide obtained by software Vesta.

(331), (422), (511), and (440), with preferential orientation in the plane (311). These values agreed with the JCPDS file 42-1467 [24]. According to Tian et al. [25], the intensity of the Co_3O_4 diffraction peak at around 44° increased slightly, identified as amorphous Co_3O_4, and the maximum intensity increased depending on the procedure used.
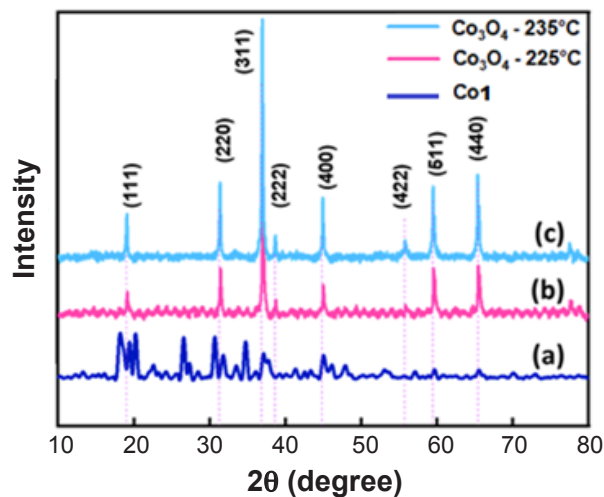

Figure 2: X-ray diffractograms for the Co_3O_4 samples obtained via sol-gel technique: a) Co1 (prior to calcination); b) Co_3O_4 calcined at 225 °C; and c) Co_3O_4 calcined at 235 °C.

In order to establish the structural parameters of the cobalt (II, III) oxide samples at the described temperatures, Rietveld refinement was carried out using the GSAS II code [26, 27]. The refined experimental data for 225 **°C** are observed in Fig. 3a where the symbols indicate the data obtained experimentally and the continuous curve

corresponds to the pattern calculated by the code. In the lower part, the solid line represents the difference between the experimental values and the simulated data, while the vertical lines indicate the angular positions of the Bragg peaks associated with the structural phase of the Co_3O_4 compound. According to the analysis process, the peak width parameters (u, v, w), the background function, scale factors, profile functions, and lattice parameters were refined. The XRD pattern shown in Fig. 3b corresponds
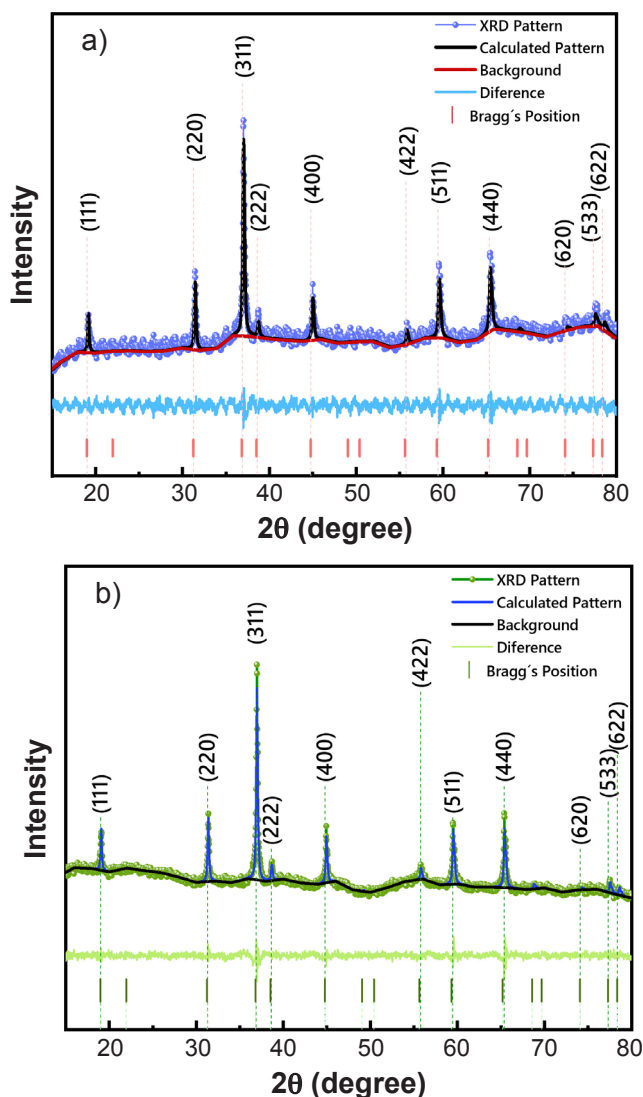

Figure 3: Refined XRD patterns for Co_3O_4 calcined at: a) 225 °C; and b) 235 °C.

to the refined experimental data for the samples obtained at 235 °C. The quality of the refinement can be verified by means of the good correspondence between the simulated and the experimental pattern and through the values of the main refinement parameters: R_{wp}= 1.47 and 1.17, and χ^2= 2.04 and 1.79 for Co_3O_4 at 225 and 235 °C, respectively.

Table I shows the structural parameters of Co_3O_4 obtained by Rietveld's refinement of the X-ray diffraction data for both temperatures. The Rietveld refinement allowed determining that Co_3O_4 crystallizes in a spinel structure with a space group Fd-3m, lattice parameters a=b=c=8.067 Å, and volume of 525.0 Å^3 for 225 °C, and a=b=c=8.071 Å and volume 525.7 Å^3 for 235 °C. The density was 6.093 and 6.186 g/cm^3, as observed in Table I. According to Ginell et al. [28], the unit cell parameters, as well as other characteristics of cobalt spinel (II, III), have some dependence on the method of sample preparation. Additional information about refinement is found in Table II. The synthesis of cobalt oxide compounds with adjustable physicochemical properties has become a recurrent research topic [29]. For the analysis of Co_3O_4, the description of the atomic positions in the spinel structure with the general formula AB_2O_4 depends on the choice of the adjustment for the origin in the space group Fd3m to which most of the spinel compounds belong [30]. Consequently, two different combinations with point symmetries 43m and 3m are possible options for the origin of the unit cell, as observed in Table II with the values obtained for the compound Co_3O_4, where the Wyckoff positions indicate the junctions for the various sites of the lattice.

The following equation was used to calculate the lattice parameter 'a' of the Co_3O_4 compound with a cubic structure centered in the faces, for 235 °C, through the analytical approach [31]:

$$\sin^2\theta = \frac{\lambda^2}{4a^2}\,(h^2 + k^2 + l^2) \qquad (A)$$

where θ is the Bragg angle of reflection and λ=1.542 Å corresponds to the wavelength for the detector with CuKα radiation. The value of a was calculated by finding the slope of the linear fit of Eq. A, using different values of h, k, l, and θ observed (Fig. 4). The slope of the linear fit obtained by regression and denoted as A was 0.00912, which in turn gave the value of the lattice parameter, a=8.073 Å.

In general, cobalt oxides have different stoichiometries and compositions based on the close thermodynamic

Table I - Structural parameters and lattice parameters of the Co_3O_4 obtained by the Rietveld refinements of the X-ray diffraction data.

Temp. (°C)	χ^2	R_{esp}	R_E	R (BS)	Rwp (BS)	GoF	a=b=c (Å)	α=β=γ	Vol. (Å^3)	Dens. (g/cm^3)
225	2.04	1.03	1.18	1.86	1.47	1.43	8.067	90°	525.0	6.093
235	1.79	0.88	0.85	1.94	1.17	1.34	8.070	90°	525.7	6.186

Table II - Information and Wyckoff positions obtained from the Rietveld refinement for the Co_3O_4.

Element	x=y=z	Site system	Wyckoff site
Co_1	0.000	-43m	4a
Co_2	0.250	-43m	16e
Co_3	0.625	3m(111)	4c
O_1	0.390	3m(111)	16e
O_2	-0.140	3m(111)	16e

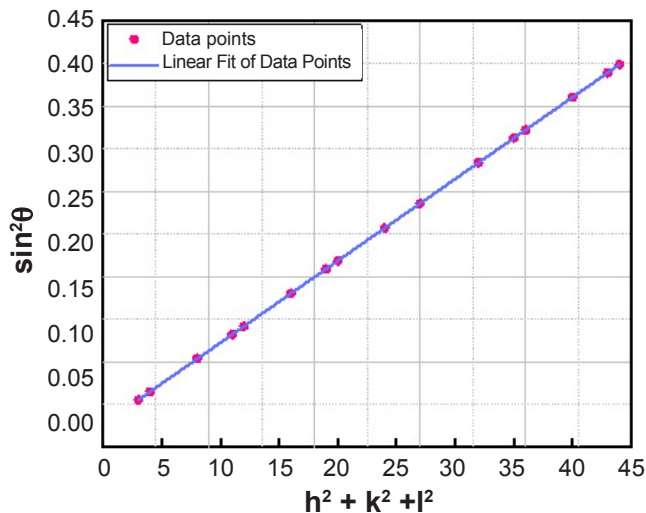|	Atom weight	Bond ratio	Angle ratio
Co^{2+}	58.93	1.45	1.25
Co^{3+}	58.93	1.45	1.25
O^{2-}	15.99	1.09	0.89

Figure 4: Variation of $\sin^2\theta$ versus $(h^2+k^2+l^2)$ for Co_3O_4 obtained by sol-gel method and calcined at 235 °C.
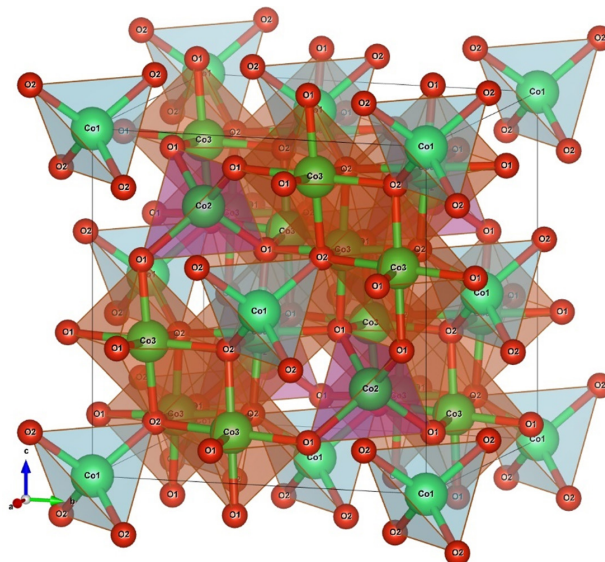

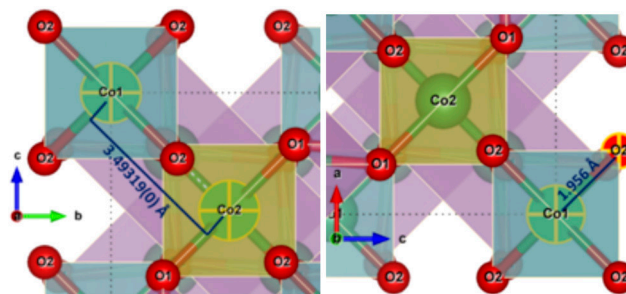Figure 5: Crystal structure of the Co_3O_4 obtained by software Vesta.

Figure 6: Interatomic distances of bonds in tetrahedra: a) Co_1-Co_2; and b) Co_1-O_2 (obtained by software Vesta).

Table III - Main inter-atomic bond lengths.

Cation	Anion	Distance (Å)
Co_1	O_2	1.956
Co_2	O_1	1.956
Co_3	O_1	1.926
Co_3	O_2	1.880

stability of the oxidation states Co^{2+} and Co^{3+}. Based on its structure, cobalt monoxide is the simplest oxide, composed of a single Co^{2+} octahedrally coordinated by the oxygen lattice in symmetry Fm3m at 300 K [19]. Fig. 5 shows the crystalline structure of the Co_3O_4 file CIF 1526734 [23] in the space group F-43m. The interatomic distance was first observed between the Co_1-Co_2 bonds, which was 3.4931 Å (Fig. 6), and between Co_1-O_2, which was 1.956 Å. Table III shows the main bond length distances, which were in the range of 1.88 and 1.956 Å. These results agreed with another study [32], where the distance of the octahedral bond was shorter than the distance of the tetrahedral bond at ambient pressure (A-O¼ 1.935 nm, B-O¼ 1.920 nm). Results also agreed with the calculated and experimental data reported in [33]. Additionally, the interatomic distances Co_3-Co_3, Co_2-Co_2, and Co_1-Co_1 were 2.794, 8.067, and 5.704 Å, respectively.

The structures of both CoO and Co_3O_4 are face-centered cubic (FCC) and are related in a simple way through their oxygen sublattices. The greatest complexity for spinel is generated from the cation distribution, which produces a decrease in the overall crystal symmetry and a larger unit cell [19]. In Table IV, the main parameters of the tetrahedra Co_1 and Co_2 and octahedron Co_3 are observed with data obtained from the refinement for the sample of cobalt oxide (II, III) at 235 °C. It was possible to identify the significant differences between the angles of inclination of the tetrahedron and octahedron, as well as the average bond length, polyhedron volume, and the x, y, and z positions of oxygen. According to Lima [34], the polyhedral volume in a spinel structure can be derived from the lattice parameter a and the oxygen position u by:

$$V_{tet} = \frac{64}{3} V\left(u - \frac{1}{8}\right) \quad\quad (B)$$

$$V_{oct} = \frac{128}{3} V\left(u - \frac{3}{8}\right)u \quad\quad (C)$$

Figs. 7a, 7b, and 7c show the SEM images of the products obtained from the sol-gel synthesis at 225 °C, 235 °C, and prior to calcination, respectively. It was observed that after calcination, agglomerated particles were formed by large and small particles with a dense stacking style, which was consistent with other researches [29, 35]. Multicomponent alloy systems, with different atomic concentrations, have complex microstructures [36]. The larger size of some particles formed was due to the excess of thermal energy absorbed by smaller particles and their interaction that generated greater agglomeration. The samples previous

to calcination showed no formation of grains or particles; the formation of an agglomerate without form, without grains, was observed instead. This was consistent with the literature indicating that the formation of particles increased with calcination [37]. According to Cardenas et al. [38], the formation of some Co-oxide structures by annealing is associated with the fusion of a thin surface layer (formed by metallic Co or CoO) that allows the dissolution of oxygen in the liquid. Some differences were observed between the samples obtained at 225 and 235 °C. The particle size was greater for the last temperature and there was a less agglomerated morphology. According to Itteboina and Sal [17], characteristics that include the topographies of the particles obtained depend on the precursors, temperature, among other factors.

Fig. 8 shows the EDS spectra and Table V shows the chemical composition of the samples obtained. Results indicated the presence of cobalt in 60% to 70%, oxygen

Table IV - Main parameters of the tetrahedron Co_1 and its distance (Å) to O_2 (a), the tetrahedron Co_2-O_1 (b), and the octahedron O_2-Co_3-O_1 (c).

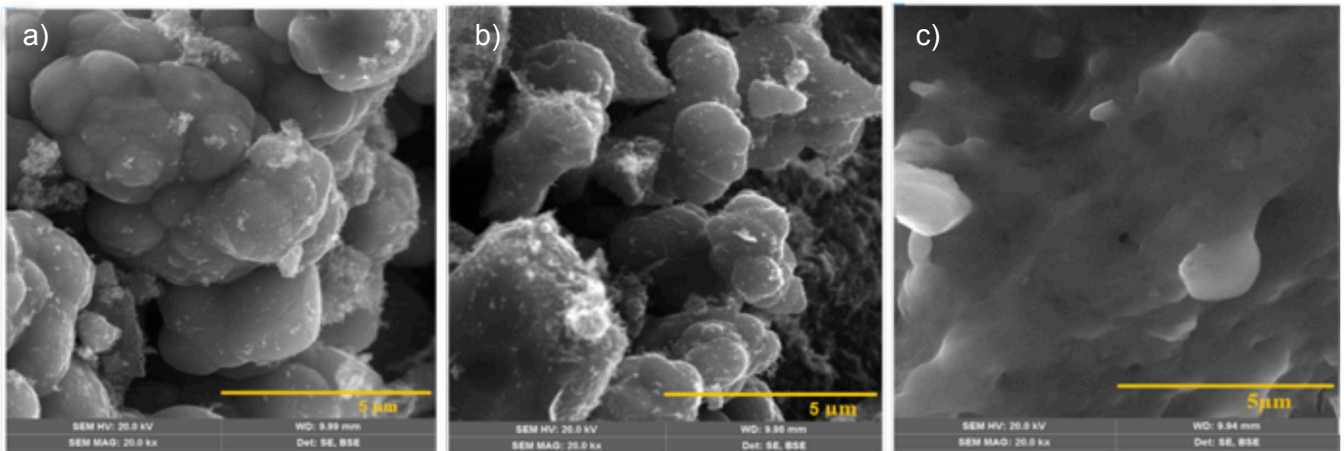| (a)				(b)				(c)			
Average bond length = 1.956 Å				Average bond length = 1.956 Å				Average bond length = 1.904 Å			
Polyhedral volume = 3.842 Å³				Polyhedral volume = 3.842 Å³				Polyhedral volume = 8.978 Å³			
	x	y	z		x	y	z	O_2	0.640	0.140	0.360
O_2	0.860	-0.140	0.860	O_1	0.610	0.610	0.390	O_2	0.860	0.140	0.140
O_2	0.860	0.140	1.140	O_1	0.610	0.890	0.110	O_2	0.860	0.360	0.360
O_2	1.140	-0.140	1.140	O_1	0.890	0.610	0.110	O_1	0.890	-0.110	0.390
O_2	1.140	0.140	0.860	O_1	0.890	0.890	0.390	O_1	0.890	0.110	0.610
								O_1	1.110	0.110	0.390

Figure 7: SEM analysis of Co_3O_4 particles obtained by sol-gel: a) calcined at 225 °C; b) calcined at 235 °C; and c) Co1 (prior to calcination).
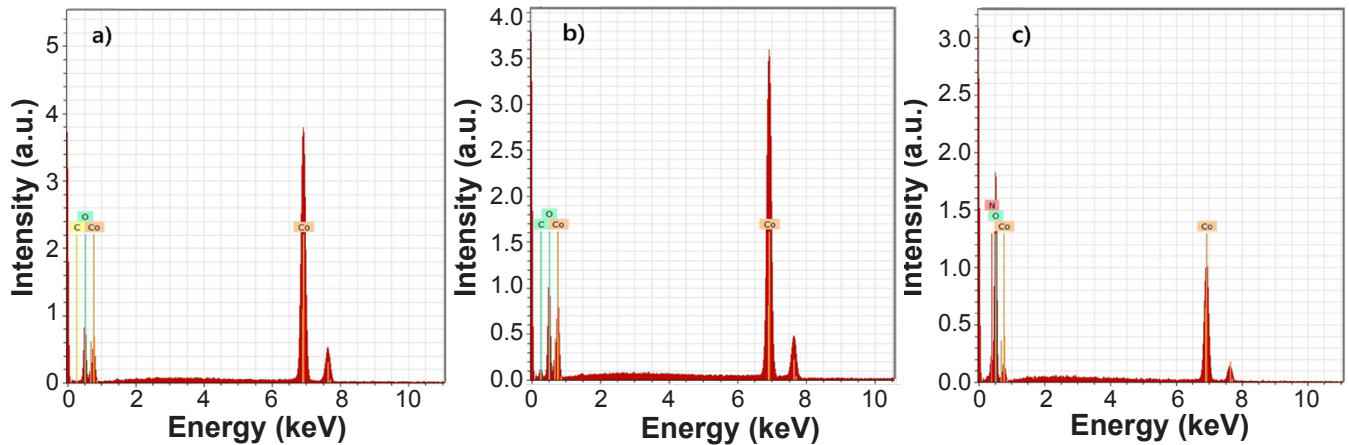
Figure 8: EDS spectra for the samples of Co_3O_4: a) 225 °C; b) 235 °C; and c) Co1.

Table V - Chemical composition (wt%) of the samples.

Element	225 °C	235 °C	Co1
Co	69.22	63.28	22.66
O	26.30	27.12	65.53
C	4.48	9.60	-
N	-	-	11.82

in ~27%, and carbon in 4% to 10% for the samples after calcination at 225 and 235 °C. For Co1, the content of cobalt was 22.7% and the presence of nitrogen was observed at 11.8%.

In Fig. 9, the particle size distributions are shown for the calcined samples where the average particle sizes (APS) for samples calcined at 225 and 235 °C were 2.37 and 2.77 μm, respectively. A slight increase in APS was observed
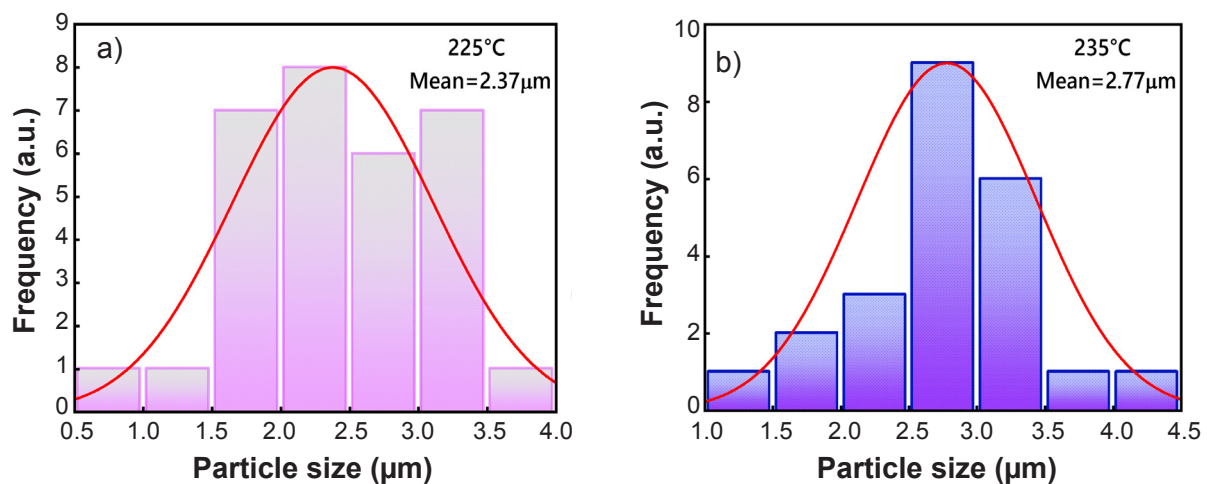

Figure 9: Particle size distribution curves of Co_3O_4 calcined at: a) 225 °C; and b) 235 °C.
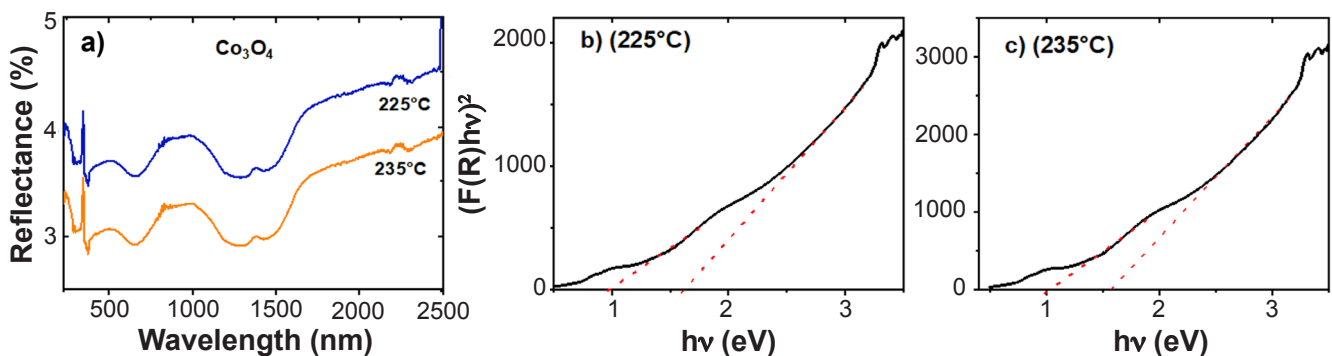

Figure 10: Reflectance spectra for samples of Co_3O_4 (a) and Tauc plots for samples calcined at 225 °C (b) and 235 °C (c).

when raising the calcination temperature. This information is relevant since the particle size and morphology of cobalt (II, III) oxide have an influence on important changes in the properties of materials [37, 39].

Fig. 10 shows the reflectance obtained through UV-vis analysis for the Co_3O_4 samples obtained by the sol-gel technique at 225 and 235 °C. The peaks are associated with the transitions of the cobalt (II, III) oxide. For the calculation of the optical band gap (E_g), the Kubelka-Munk method was used through the following equation to calculate the value of F(R) [40]:

$$F(R) = \frac{1-R^2}{2R} \tag{D}$$

where R is the reflectance and F(R) is the Kubelka-Munk function. The band gap calculation can be approximated by extrapolating the linear region from the graph F(R).h.ν vs. h.ν (photon energy), resulting in 1.6 eV for the first region and 0.97 eV for the second one. This can be attributed to the charge transfer of O^{2-}-Co^{2+} and O^{2-}-Co^{3+} [10]. The intensity of the Co_3O_4 peaks in UV-vis changed with the calcination temperature of the samples, increasing at higher temperatures [41].

CONCLUSIONS

The synthesis of cobalt oxide Co_3O_4 was carried out by means of the sol-gel technique with subsequent calcination at 225 and 235 °C. Rietveld refinement of the XRD patterns of the samples obtained was carried out. It was determined that this compound crystallizes in the FCC structure, space group Fd-3m, with main values of GoF of 1.43 and 1.34, with lattice parameters of 8.06 and 8.07 Å, a volume of 525.0 and 525.7 Å^3, and a density of 6.093 and 6.186 g/cm^3 for the 225 and 235 °C samples, respectively. The lattice parameter calculation obtained through the analytical approach for the 235 °C sample was 8.073 Å, which coincided with that calculated by means of Rietveld. The interatomic distances were analyzed, as well as the main parameters of the Co_1, Co_2, and Co_3 polyhedra and inclination angles with data obtained from the refinement. The average length of the Co_1 and Co_2 tetrahedra was 1.956 Å and the volume was 3.842 Å^3, while for the octahedron of Co_3 the length was 1.904 Å and the volume was 8.978 Å^3. These results allowed establishing the structural behavior of Co_3O_4 when the temperature was varied, and thus its effect was evaluated. Through scanning electron microscopy, the mean grain size was established in 2.37 and 2.77 μm for samples calcined at 225 and 235 °C, respectively; agglomerated particles and a dense stacking resulting from the effect of temperature were observed. UV-vis analysis allowed determining the value of the band gap (E_g) in the first and second region with values of 1.6 and 0.97 eV, respectively.

ACKNOWLEDGEMENTS

REFERENCES

[1] X. Wang, L. Yu, P. Hu, F. Yuan, Cryst. Growth Des. **7** (2007) 2415.
[2] Y.F. Liu, J.L. Xie, M. Luo, B. Peng, L.J. Deng, Mater. Sci. Forum **898** (2017) 1561.
[3] X. Wang, W. Tian, T. Zhai, C. Zhi, Y. Bando, J. Mater. Chem. **22** (2012) 23310.
[4] A. Numan, M.M. Shahid, F.S. Omar, K. Ramesh, S. Ramesh, Sens. Actuators B Chem. **238** (2017) 1043.
[5] Y. Lu, T. Liu, C. Dong, C. Huang, Y. Li, J. Chen, S. Wang, J. Adv. Mater. **33**, 8 (2021) 2007056.
[6] H. Karimi-Maleh, M.L. Yola, N. Atar, Y. Orooji, F. Karimi, P. Kumar, M. Baghayeri. J. Colloid Interface Sci. **592** (2021) 174.
[7] Y. Fu, X. Guo, Z. Xu, G. Zhao, C. Xu, Y. Zhu, L. Zhou, ACS Appl. Mater. Interfaces, *in press*.
[8] S.P. Keerthana, R. Yuvakkumar, P.S. Kumar, G. Ravi, D. Vo, D. Velauthapillai, Chemosphere **277** (2021) 130325.
[9] L.J. Cardenas-Flechas, P.T.C. Freire, E.C. Paris, L.C. Moreno, M.R. Joya, Materialia **18** (2021) 101155.
[10] L.J. Cardenas-Flechas, A.M. Raba, J. Barba-Ortega, L.C. Moreno, M.R. Joya, J. Inorg. Organomet. Polym. Mater. **30** (2020) 1.
[11] J. Guo, L. Chen, X. Zhang, B. Jiang, L. Ma, Electrochim. Acta **129** (2014) 410.
[12] A.B. Vennela, D. Mangalaraj, N. Muthukumarasamy, S. Agilan, K.V. Hemalatha, Int. J. Electrochem. Sci. **14** (2019) 3535.
[13] S. Sadasivan, R.M. Bellabarba, R.P. Tooze, Nanoscale **5** (2013) 11139.
[14] S.G. Victoria, A.M.E. Raj, C. Ravidhas, Mater. Chem. Phys. **162** (2015) 852.
[15] J. Chen, Z. Xu, H. Zhu, R. Liu, X. Song, Q. Song, H. Cui, Vacuum **174** (2020) 109219.
[16] T.K. Sau, A.L. Rogach, Adv. Mater. **22** (2010) 1781.
[17] R. Itteboina, T.K. Sal, Mater. Today Proc. **9** (2019) 458.
[18] B. Raveau, M. Seikh, *Cobalt oxides: from crystal chemistry to physics*, Wiley (2012) 3.
[19] S.C. Petitto, E.M. Marsh, G.A. Carson, M.A. Langell, J. Mol. Catal. A Chem. **281** (2008) 49.
[20] A. El Abed, S.E. Elqebbaj, M. Zakhour, M. Champeaux, J.M. Perez-Mato, J. Darriet, J. Solid State Chem. **161** (2001) 300.
[21] S. Saito, K. Nakahigashi, Y. Shimomura, J. Phys. Soc. Jpn. **21** (1966) 850.
[22] J.M. Tarascon, G. Vaughan, Y. Chabre, L. Seguin, M. Anne, P. Strobel, G. Amatucci, J. Solid State Chem. **147** (1999) 410.
[23] I.S. Kotousova, S.M. Polyakov, Kristallografiya **17** (1972) 661.
[24] R. Jiang, L. Jia, X. Guo, Z. Zhao, J. Du, X. Wang, F. Xing, Sens. Actuators B Chem. **290** (2019) 275.
[25] R. Tian, H. Dong, J. Chen, R. Li, Q. Xie, Sep. Purif. Technol. **250** (2020) 117246.
[26] M. Farahmandjou, Phys. Chem. Res. **4** (2016) 153.
[27] B.H. Toby, R.B. Von Dreele, J. Appl. Crystallogr. **46**

(2013) 544.

[28] K.M. Ginell, C. Horn, R.B. Von Dreele, B.H. Toby, Powder Diffr. **34** (2019) 184.

[29] C. Suryanarayana, M.G. Norton, *X-ray diffraction*, Springer, Boston (1998) 63.

[30] L.J. Cardenas-Flechas, A.M. Raba, M. Rincón-Joya, Dyna **87** (2020) 184.

[31] O. Knop, K.I.G. Reid, Sutarno, Y. Nakagawa, Can. J. Chem. **46** (1968) 3463.

[32] K.E. Sickafus, J.M. Wills, J. Am. Ceram. Soc. **82** (1999) 3279.

[33] S. Hirai, W.L. Mao, Appl. Phys. Lett. **102** (2013) 41912.

[34] A.F. Lima, J. Phys. Chem. Solids **75** (2014) 148.

[35] L. Bai, M. Pravica, Y. Zhao, C. Park, Y. Meng, S.V. Sinogeikin, G. Shen, J. Phys. Condens. Matter. **24** (2012) 435401.

[36] B. Liu, X. Zhang, H. Shioyama, T. Mukai, T. Sakai, Q. Xu, J. Power Sources **195** (2010) 857.

[37] J. Cardenas, J. Leon, J.J. Olaya, Corros. Eng. Sci. Technol. **54** (2019) 233.

[38] L. Cardenas, J. Barba-Ortega, M.R. Joya, Rev. UIS Ing. **19** (2020) 171.

[39] C. Maurizio, R. Edla, M. Orlandi, A. Trapananti, G. Mattei, A. Miotello, Appl. Surf. Sci. **439** (2018) 876.

[40] G.A. Babu, G. Ravi, Y. Hayakawa, M. Kumaresavanji, J. Magn. Magn. Mater. **375** (2015) 184.

[41] M.F. Valan, A. Manikandan, S.A. Antony, J. Nanosci. Nanotechnol. **15** (2015) 4580.